Dear

Please find attached a PDF of your article that has appeared in issue   of Physica Scripta. This file has been optimised for viewing on screen, but can be printed off. If you would like a version of this file, optimised for printing, or would like to purchase a number of printed copies of your paper, please contact me.

Best Wishes,

Audrey Samuels
Journal Controller
Marston Digital
Omega Park
Collet
Didcot
OX11 7AW
email: samuelsa@lrl.com
voice: +44 1235 518700
fax: +44 1235 515777
web: http://www.physica.org

Modeling of the Diffusion of Hydrogen in Porous Graphite

Manoj Warrier[1,*], Ralf Schneider[1], Emppu Salonen[2,**] and Kai Nordlund[2]

[1] EURATOM Association, Max-Planck-Institut für Plasmaphysik, Teilinstitut Greifswald, Wendelsteinstrasse 1, D-17491 Greifswald, Germany
[2] Accelerator Laboratory, P.O.Box 43, FIN-00014, University of Helsinki, Finland

Abstract

The graphite used in fusion devices as first wall material is porous and consists of granules and voids [1,2]. The 1–10 μm granules are further composed of graphitic micro-crystallites (5–10 nm), which are separated by micro-voids. Understanding the hydrogen transport and trapping in such granules is an important aspect of understanding the effect of a realistic graphite structure on hydrogen recycling and hydrocarbon formation in graphite. We use Kinetic Monte Carlo (KMC) to study the diffusion of hydrogen in a typical granule of graphite. We use molecular dynamics (MD) to obtain the jump attempt frequency ω_o and the migration energy E_m of interstitial graphite which are inputs to the KMC. A consistent parameterization of MD within KMC is presented. The diffusion shows a non-Arrhenius behavior which can be explained with two types of different jump processes within the graphite crystal. The porous granule structure is constructed using statistical distributions for the crystallite dimensions and for crystallite orientations at a given porosity. The hydrogen trapping at inter-crystallite micro-voids are modeled by assuming that a fraction of the hydrogen atom flux transiting through the micro-void is trapped. We present a parametric study of the diffusion and trapping of hydrogen within the granule for various trapping fractions at the inter-crystallite micro-voids.

1. Introduction

Graphite is a widely used plasma facing material in fusion devices mainly due to its properties of having a low atomic number, good thermal conductivity, a high sublimation temperature, easy handling and machining, etc. However, it is highly chemically reactive and porous. This results in large chemically reacting internal surfaces which the hydrogen isotopes can diffuse into, recombine or form hydrocarbons and get trapped in the bulk of the graphite ([1–5] and references therein). Moreover, when making the transition to reactor relevant fusion machines with long pulse times, tritium co-deposition and recovery is so serious an issue that other plasma facing materials are considered instead of graphite or Carbon Fiber Composites (CFCs) [6,7]. There exist some very good semi-empirical models for chemical erosion [4,8] which are fitted to experimental results. However, there exists a factor of two scatter in general in the experimental results due to different material structures and different methods of measurement [8]. There is also uncertainty about the extrapolation of the chemical sputtering yield to high reactor relevant fluxes, and in accounting for higher hydrocarbon formation [9]. There is also great disparity in the diffusion data of hydrogen isotopes in graphite [10]. Understanding the effects of porosity, trapping inside granules or at internal surfaces,

the various chemical interactions that can occur within graphite, and the transport of hydrogen and the molecules formed is essential to interpret existing experimental results and to design new types of graphite which are better suited as fusion reactor first wall materials.

Several analytical phenomenological models have been proposed for hydrogen recycling from graphite. Möller and Scherzer [1] and Haasz et al. [2] have proposed detailed models for hydrogen recycling wherein they have included the different channels of hydrogen diffusion in porous graphite by assigning different rates of transport for the diffusing hydrogen in different regions (trans granule diffusion and diffusion through the internal surfaces bounding the porous regions). However, these models do not include hydrocarbon formation. Mech et al. [4] and Küppers et al. [5] have included rates for hydrocarbon formation (mainly methane) for hydrogen interaction with graphite, but do not look at the hydrogen recycling nor at the porous structure of graphite. Hassanein et al. [11] and Federici and Wu [3] have looked at the problem of tritium diffusion in redeposited layers of "candidate" fusion reactor plasma facing materials. These redeposited layers too have a porous structure and different hydrogen diffusion channels just like graphite. In this paper we look at hydrogen diffusion in a granule of graphite (trans granular diffusion) as part of a bigger campaign to create simulation codes for studying hydrogen isotope diffusion in porous "candidate" plasma facing materials for fusion reactors.

An illustration of the porous structure of graphite is shown in Fig. 1. It consists of granules of size around a few microns piled on top of each other with gaps (voids) in between. The size of the voids are typically of the order of 0.1 μ. The granules themselves are made up of crystallites (regions of crystal graphite) which are of the order of a few nanometers wide. The crystallites are separated by micro-voids which are a few Ångströms wide [1,2]. Therefore, as we can see there is a large difference in length scales for hydrogen diffusion depending on the region of graphite it is in. We use molecular dynamics (MD) to simulate the diffusion of a hydrogen interstitial in a graphite crystal at different temperatures. By analyzing the trajectory of the interstitial hydrogen graphite, we can obtain information about its diffusion coefficient and also information about its transport that can be used in a Kinetic Monte Carlo (KMC) ansatz [12] to model the diffusion of much larger numbers of hydrogen atoms over a much larger space domain and also allows one to simulate processes with widely varying time scales.

In the next section we describe the MD and results for hydrogen interstitial diffusion in a graphite crystal and also

* To whom correspondence should be addressed: e-mail: Manoj.Warrier@ipp.mpg.de.Permanent address: Institute for Plasma Research, BHAT, Grandhingar, Gujarat, India-382428.
**Present Address: Laboratory of Physics, Helsinki University of Technology, P.O. Box 1100, FIN-02015 HUT, Finland.
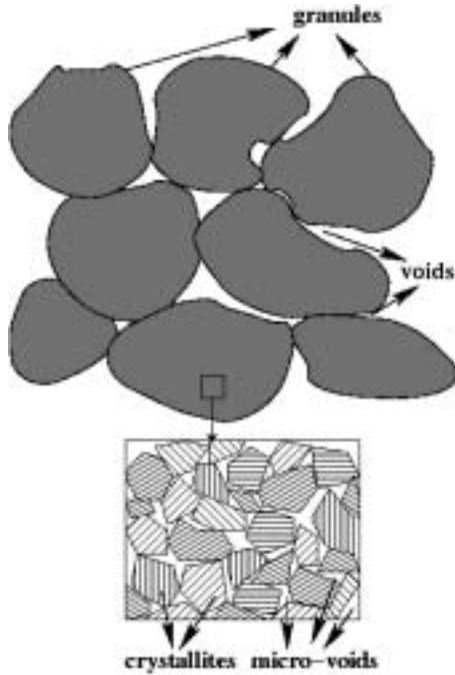
Fig. 1. The porous structure of graphite.

the analysis of hydrogen trajectories to provide inputs to the KMC. In the third section we describe an algorithm to create a porous structure which can either be granules and voids or crystallites and micro-voids. Then in the fourth section we describe the KMC runs and results for hydrogen diffusion in a granule of graphite. Finally we provide conclusions and plans for future work.

2. Molecular dynamics study of hydrogen diffusion in graphite

We use the HCParcas code to study hydrogen diffusion in crystalline graphite. The code uses the Brenner potential [13] with the Nordlund long range interaction term [14] to simulate a graphite crystal. The simulations consist of a single hydrogen interstitial diffusing in a graphite crystal consisting of 960 atoms at different temperatures of graphite (150 K, 300 K, 450 K, 600 K, 750 K and 900 K). Periodic boundary conditions are applied along X, Y and Z in all the simulations described below.

2.1. Setting up the simulation

The graphite crystal samples are prepared by starting with 960 carbon atoms at the graphite crystal locations. These atoms are then maintained at their respective temperatures by means of a Berendsen thermostat [15]. It is checked that the lowest potential energy state is reached and also that the pressure oscillates around zero. The hydrogen interstitial (henceforth referred to as interstitial, unless otherwise specified) is created by randomly picking a position inside the graphite crystal and making sure that it is more than a given distance from any of the carbon atoms constituting the graphite lattice. It is given zero initial velocity. The simulation at each temperature is run for 100 pico seconds with a time step of the order of a femto second. It is assumed that the interstitial equilibrates with the graphite crystal in a couple of pico seconds. The interstitial vibrates (attempts to jump) in the potential well

of the vibrating carbon atoms and makes a jump from one potential well to another depending on the depth of the well (migration energy barrier) and the graphite temperature. There occurs at least 200 (at 150 K) such jump events during the course of a 100 ps simulation. We therefore feel that a 100 ps simulation is sufficient to provide equilibration and statistics to analyze the interstitial diffusion in the graphite crystal. We output the interstitial trajectories at each time step for analysis of the interstitial diffusion.

2.2. Results and analysis

We observe that the interstitial does not show any cross graphene layer diffusion at any of the graphite temperatures simulated. The position of the interstitial is output at every time step of the MD code and the trajectory is analyzed to create inputs for the KMC code. Specifically what is needed for KMC is the jump attempt frequency ω_o, the migration energy E_m, and the jump distance L_i. It is assumed that the interstitial trajectory is diffusive and the diffusion is represented by

$$\omega = \omega_o e^{-E_m/k_b T} \qquad (1)$$

where, ω is the jump frequency, the frequency with which the interstitial jumps a distance L_j in a specified direction and k_B is the Boltzmann's constant.

It is essential to keep in mind that the MD time step is short enough so that the interstitial experiences only a fractional change in potential energy for numerical stability when solving for the force equation. Therefore, one can expect the direction of the interstitial to be randomized only after several MD time steps, or equivalently after only a certain length dr. For a random walk with equal probability of taking a step in any direction the expectation value of the mean square displacement is $N \times dr^2$, where N is the number of steps. For our fixed time (100 ps) interstitial trajectories, as dr is increased the number of jumps N (defined here as the number of times the interstitial displaces by a distance dr) decreases. Therefore, to determine at what value of dr the trajectory is randomized, we plot $N \times dr^2$ as a function of dr. The value of dr for which $N \times dr^2$ gets saturated is taken as L_j and the corresponding value of N is taken as ω. This analysis is carried out for interstitial trajectories at different temperatures and Eq. (1) is used to fit the data to obtain ω_o and E_m. We see mainly diffusion with a short step-size at all target temperatures, with a long step-size diffusion making its appearance at higher temperatures (≥ 450 K).

A plot of $N \times dr^2$ vs. dr is shown in Fig. 2 for the hydrogen interstitial trajectories in a perfect graphite crystal from the MD code HCParcas at different graphite temperatures. We see that at lower temperatures (≤ 450 K) a saturation of $N \times dr^2$ is seen at $dr = 2.5$ Å. At higher temperatures, the saturation occurs at larger values of dr. Note that the saturation threshold is lower for the 750 K case as compared to the 600 K case. The 900 K case does not saturate at all. The different diffusion length steps are included as different jump processes when we do the Arrhenius fit for obtaining ω_o and E_m. For the numerical fitting we assume a sum of two diffusive processes, one with a low jump attempt frequency ω_o^l and low migration energy barrier E_m^l and the other with a high jump attempt frequency ω_o^h and a high migration energy barrier E_m^h. In
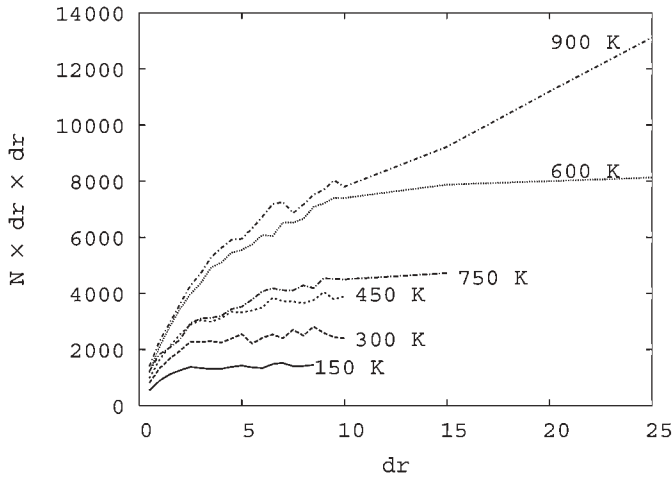
Fig. 2. Analysis of $N \times dr^2$ for hydrogen interstitials.

the next paragraph we discuss the various diffusion pathways of interstitials in graphite.

The various possible jump paths of a interstitial hydrogen in a graphite crystal is illustrated in Fig. 3. The squares and circles represent carbon atoms lying on separate graphene layers which sandwich the interstitial. The interstitial occupies the large gap between the graphene layers and as mentioned above cannot squeeze through the graphene layer. The lowest energy state for the interstitial seems to lie below the center of the hexagons that constitute the graphene layer. The easiest pathway for diffusion is from below the center of one hexagon to above the center of the neighboring hexagon lying on the opposite graphene layer (denoted by **HB** in Fig. 3). Another possibility is the jump from below the center of one hexagon to the center of the neighboring hexagon on the graphene layer (denoted by **HA** in Fig. 3). Note that one
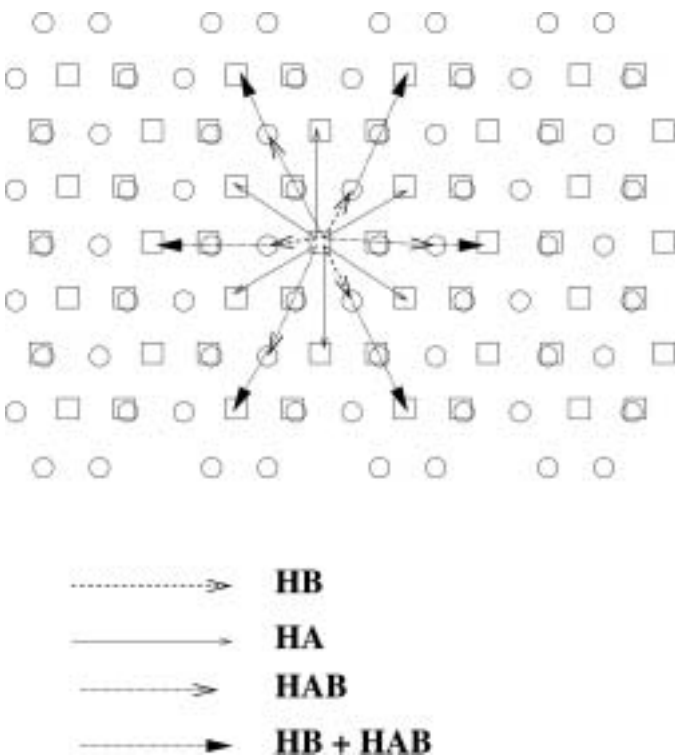

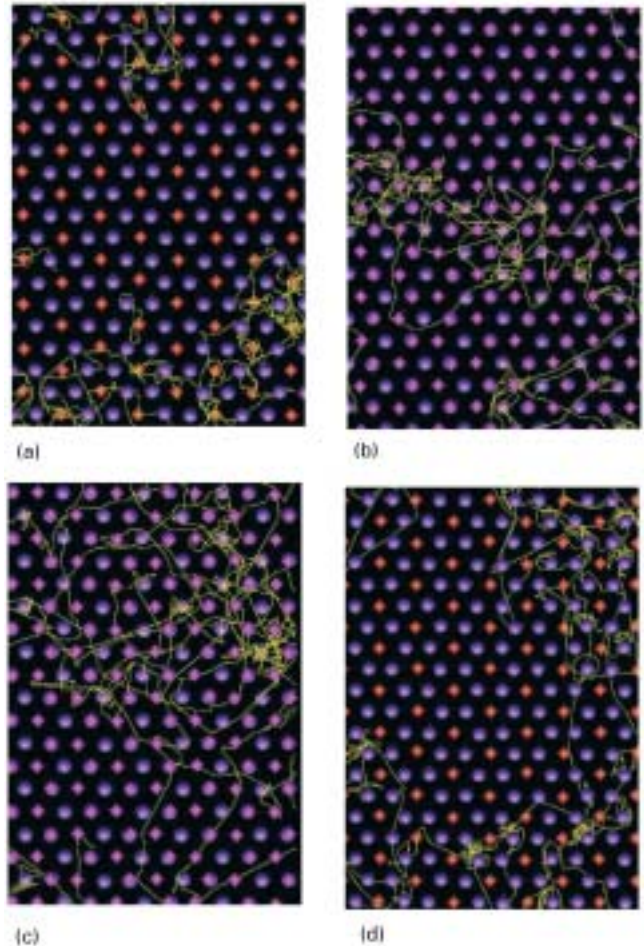*Fig. 3.* Various possibilities for interstitial jumps in a graphite crystal.

Fig. 4. Interstitial trajectory at (a) 300 K, (b) 450 K, (c) 600 K and (d) 750 K from MD.

HA jump is achieved with two consecutive **HB** jumps. Other possibilities for diffusion pathways which have longer step lengths are **HAB** and combinations of the **HB** + **HAB** types. From our simulations we find that **HB** and **HA** jumps are the main diffusion pathways at low temperatures (Fig. 4) below 450 K and that jumps of the type **HAB** and **HB** + **HAB** start contributing to the diffusion coefficient at temperatures above 450 K (Fig. 4). This can be easily understood when we look at the sum of two Arrhenius fits we use to fit the jump counts obtained from the MD simulations at different temperatures. We see (Fig. 5) that the values $E_m^l = 0.0147\,\text{eV}$, $\omega_o^l = 6.84 \times 10^{12}\,\text{s}^{-1}$, $E_m^h = 0.269\,\text{eV}$ and $\omega_o^h = 2.74 \times 10^{13}\,\text{s}^{-1}$ match the MD results. What this means is that the interstitials usually have jumps of the type **HA**, or **HB**, or a combination of the two, because of the low migration energy associated with these jumps (comparable to or lesser than the temperature of the interstitials). At higher temperatures they also have a probability to make jumps of the **HAB** type where they can also squeeze between two carbon atoms oscillating on opposing graphene layers. We do not explain the increased jump count at 600 K with this model. However, based on the saturation threshold of $N \times dr \times dr$ for 600 K, we speculate that it is the higher step-size at 600 K that causes it. Using a higher step-size in the KMC, reproduces the resulting larger diffusion coefficient at 600 K.
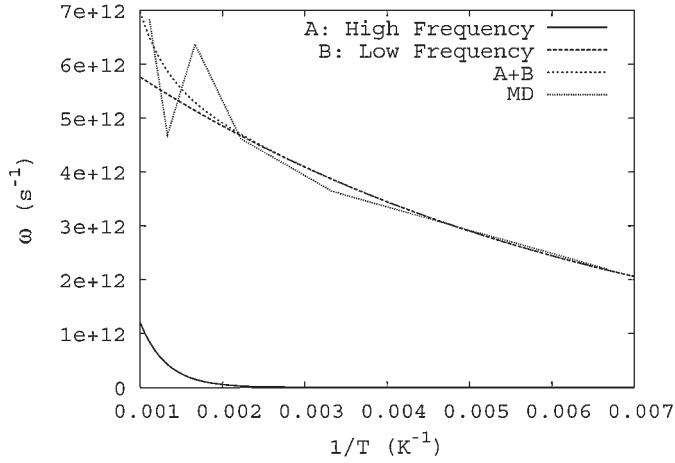
Fig. 5. Sum of two Arrhenius fits to the interstitial jump counts from MD.

3. Creating a porous graphite structure

An algorithm "inspired" by F. Graziani's algorithm to create a mixture of two different elements in an alloy [16] is employed to create the porous graphite structure. It can be used to create either a graphite sample made of granules and voids or a granule of graphite made up of crystallites and micro-voids.

The void fraction, physical dimensions of the region being modeled, mean dimensions of the sub-structure (either granules or crystallites), size of a simulation cell (typically 0.1 times the size of the sub-structure) and the smoothness of the sub-structure are input. Uniformly distributed random numbers are used to pick up a random point P within the region being modeled. The substructure is constructed around P. This is done using a Poisson random number distribution with a mean corresponding to the sub-structure dimensions along X, Y and Z, with a selection process to maintain the required smoothness of the substructure. After the construction of a substructure it is checked if the fraction of voids is greater than the specified void fraction. If yes, a new substructure is added as described above. If no, the structure is written out in a graphite structure file which is nothing but a 3-D grid with regions occupied by voids and sub-structures.

If the sub-structure are crystallites, then one would also assign orientations of the crystallites. This is done by specifying the Euler angles ϕ, θ and ψ [17] of rotation for
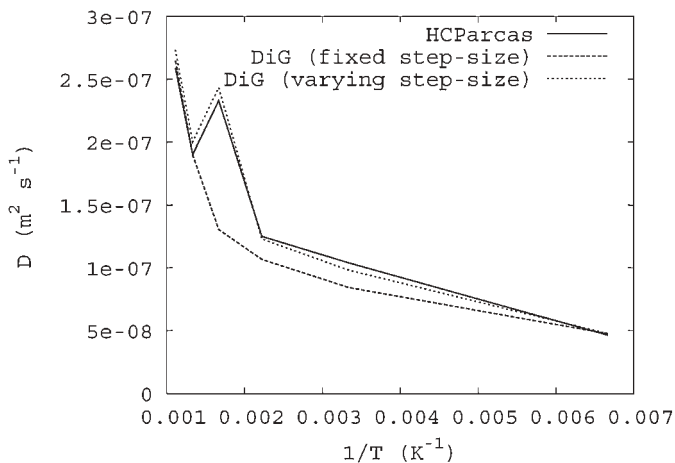

Fig. 6. Diffusion coefficient of hydrogen interstitial in pure crystal graphite: Comparision of KMC with MD.

each crystallite with respect to a crystallite oriented along the Z direction. Care should be taken to make sure that neighboring crystallites do not have very different orientations. At present we do this by specifying ϕ, θ and ψ as inputs and adding minor corrections which are again Poisson distributions with mean values $d\phi$, $d\theta$ and $d\psi$.

4. KMC of hydrogen interstitial in porous graphite

A KMC code is being developed to study the diffusion of interstitials in graphite. It is written in a modular fashion to make addition of new species, new interactions, etc., easy. As an initial implementation, the above acquired $\omega_o^l, E_m^l, \omega_o^h$ and E_m^h were used to study the diffusion of hydrogen in (a) pure, crystalline graphite and (b) graphite with crystallites and voids. The results from (a) for the diffusion coefficient of hydrogen interstitial in graphite are compared with the MD results. In case (b), a simple model for trapping and transport at the voids has been implemented and the variation in the diffusion coefficient with the void fraction and trapping probability is studied.

4.1. *Comparison of the diffusion coefficient with the MD results*

We use the values obtained from the MD interstitial trajectory analysis, $\omega_o^l = 6.84 \times 10^{12}\,\text{s}^{-1}$, $E_m^l = 0.0148\,\text{eV}$, $\omega_o^h = 2.74 \times 10^{13}\,\text{s}^{-1}$ and $E_m^h = 0.269\,\text{eV}$ as inputs to the KMC code. In Fig. 6 we compare the values for diffusion coefficient for hydrogen interstitial in pure crystalline graphite from the KMC code with the results from MD in two cases, (1) with constant step lengths (3.5 Å) for the smaller step and 12 Å for the larger step size gives best results) and (2) with the step sizes varying so as to be in the diffusive regime always as dictated by Fig. 2. We see generally a good agreement between between the MD and KMC in both cases, except for a mismatch of less than a factor of 2 for the 600 K in case (1). This mismatch disappears in the varying step size case.

4.2. *Effect of trapping probability and void fraction on the diffusion coefficient*

We keep the above inputs to the KMC fixed and use a varying step size (best fit as obtained in the previous section) and study the effect of different trapping probabilities and void fractions on the diffusion coefficient of the hydrogen interstitial in porous graphite. We use a very simple void model for our present study. When an interstitial reaches a void it can get trapped with a specified trapping probability. This trapping probability should depend upon how saturated the void is, but we treat it as an input at present and study the effect of varying this parameter on the diffusion coefficient. The interstitials that do not get trapped continue on their way (they just take a long step) till they reach a non-void region. We also do not include detrapping of the trapped interstitials in the present model. This is a valid assumption since the reported trap energies (4.3 eV [10]) are much higher than E_m^h and E_m^l and the detrapping attempt frequency is expected to be of the order of phonon frequencies $\simeq 1 \times 10^{13}\,\text{s}^{-1}$, which is of the same order as ω_o^h and ω_o^l. We study the diffusion coefficient of the interstitial with the void fraction as the varying parameter at different graphite temperatures. However, we would like
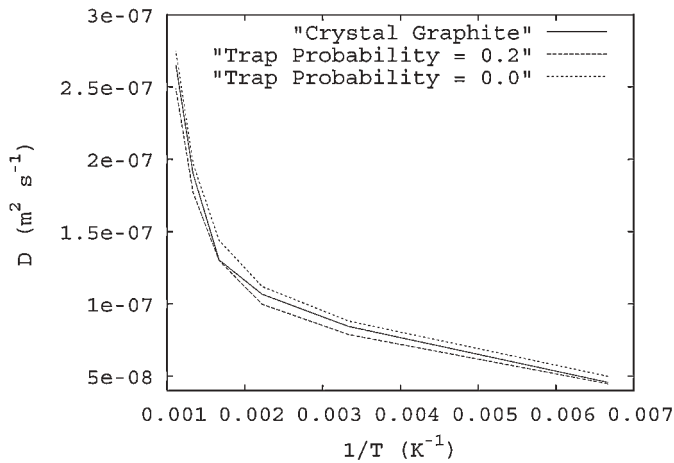
Fig. 7. Diffusion coefficient at a void fraction 10% compared with that for crystal graphite at two different trap probabilities.

to emphasize that a more rigorous model (with a better transport model within voids and with detrapping included) is needed for treating the voids.

A plot of the diffusion coefficient of the interstitials for a void fraction of 10% for no trapping and for a trapping probability of 0.2 has been compared with that for pure crystal graphite in Fig. 7. We see that the diffusion coefficient increases due to the presence of voids and that it decreases when trapping is introduced.

5. Conclusions and discussion

We have developed a KMC code that simulates the diffusion of interstitials in porous graphite and match the results for hydrogen diffusion in pure crystal graphite as obtained from MD. We show that this diffusion shows a non-Arrhenius behavior due to the existence of two different jump mechanisms, one with a low jump attempt frequency and low migration energy barrier which is dominant at the temperatures studied, and the other which has a high jump attempt frequency and a high migration energy barrier which starts contributing to the diffusion above 450 K. We use a simple void model to do parametric studies of the diffusion in porous graphite with the trapping probability at the voids being the varying parameters.

The mechanism for enhanced diffusion at 600 K is not clear and it is speculated that larger step-size of diffusion is the effect that drives it. However the cause of the larger step-size needs further analysis.

Acknowledgments

References

1. Möller, W., J. Nucl. Mater. **162–164**, 138 (1989).
2. Haasz, A. A., Franzen, P., Davis, J. W., Chiu, S. and Pitcher, C. S., J. Appl. Phys., 77(1): 66–86 (1995).
3. Federici, G. and Wu, C. H., J. Nucl. Mater. **186**, 131 (1992).
4. Mech, B. V., Haasz, A. A. and Davis, J. W., J. Appl. Phys. **84**, 1655 (1998).
5. Küppers, J. Surf. Sci. Rep. **22**, 249 (1995).
6. Federici, G. *et al.*, J. Nucl. Mater. **266–269**, 14 (1999).
7. Janeschitz, G., ITER JCT, and HTs. J. Nucl. Mater. **290–293**, 1 (2001).
8. Roth, J., J. Nucl. Mater. **266–269**, 51 (1999).
9. Federici, G. *et al.*, Nucl. Fusion, #**12R**, 1967 (2001).
10. Wilson, K. L. *et al.*, "Atomic and plasma-material interaction data for fusion," (suppl. to Nucl. Fusion) **1**, 31 (1991).
11. Hassanein, A., Wiechers, B., and Konkashbaev, I., J. Nucl. Mater. **258–263**, 295 (1998).
12. Bortz, A. B., Kalos, M. H., and Lebowitz, J. L., J. Comput. Phys. **17**, 10 (1975).
13. Brenner, D. W., Phys. Rev. B **42**, 9458 (1990).
14. Nordlund, K., Keinonen, J. and Mattila, T., Phys. Rev. Lett. **77**, 699 (1996).
15. Berendsen, H. J. C., Postma, J. P. M., van Gunsteren, W. F., DiNola, A. and Haak, J. R., J. Chem. Phys. **81**, 3684 (1984).
16. Graziani, F., "APS Meeting: Conf. Computational Phys. 2002, August 25–28 (San Diego, 2002).
17. Goldstein, H., "Classical Mechanics," (Addison Wesley Publishing Co., 1971), p. 317.